Journal of Civil Engineering and Architecture 15 (2021) 57-62
doi: 10.17265/1934-7359/2021.02.001

Beam Element Material Model for Rotary-Straightened Steel W-Shapes

Barry T. Rosson

Department of Civil, Environmental and Geomatics Engineering, Florida Atlantic University, Boca Raton, FL 33431, USA

Abstract: An inelastic material model that was previously developed by the author for standard W-Shapes was adapted for use to model the behavior and strength of rotary-straightened hot rolled W-Shape sections. Using a published residual stress model for these W-Shapes, limit load analyses were conducted using the material model in MASTAN2 and were compared with published finite element results. The material model required an adjustment to the initial yield moment conditions and residual stress ratios. Comparisons with published results indicate that these minor modifications were sufficient to provide very good modeling agreement. The previously developed material model can be used effectively to model the limit load conditions of rotary-straightened hot rolled W-Shape beams and beam-columns in steel frames. The effect of rotary-straightening W-Shapes is more significant for minor axis bending conditions and this becomes more pronounced as the floor load magnitudes increase.

Key words: Nonlinear analysis, steel buildings, stiffness reduction, material model.

1. Introduction

Since the early 1970's, it has been known that roller-straightening hot rolled W-Shapes increases the column strength on the order of 10 to 20 percent in the L/r range of 40 to 100 [1]. This is due primarily to the fact that the rotarizing process removes, or greatly reduces, the compressive residual stresses at the flange tips for most steel columns that were manufactured during that time period. Since then, modern manufacturing processes have greatly improved, with equipment and procedures that currently permit rotary-straightening of sections with a weight of almost 400 lb/ft and depths up to 36 inches; thus, most sections are now rotarized [2]. For compact W-Shapes with an ECCS (European Convention for Constructional Steelwork) residual stress distribution pattern [3], the stiffness reduction that results from yielding of the cross-section due to uniaxial bending and axial compression has been studied in detail for several years [4, 5]. Three-dimensional m-p-τ surface plots were used to discuss the stress states around the perimeter of the surfaces and to develop an inelastic material model in MASTAN2 [6] that was accurate and easy to use when determining the limit load capacity of beam-columns and frames [7-9]. Further development of the inelastic material model included the enhancement of normalized tangent modulus expressions in MASTAN2 for combined major axis and minor axis beam bending conditions using a 14-DOF beam element to determine the lateral-torsional buckling capacity of rolled I-section beams [10]. The objective of this study is to demonstrate that the previously developed inelastic material models can be adapted for use in modeling the nonlinear behavior of rotary-straightened hot rolled W-Shapes.

Corresponding author: Barry T. Rosson, Ph.D., professor, research field: nonlinear structural steel behavior.

2. Stiffness Reduction Model

As previously demonstrated by Rosson et al. [7-9], the extent of $\tau = 1$ for W-Shapes with an ECCS residual stress pattern [3] is determined when the moment and axial load conditions cause all three compression stresses at the flange ends to sum to σ_y. The maximum moment at which $\tau = 1$ is maintained

for minor axis bending is given as

$$m_1 = \frac{S_y}{Z_y}(1 - c_r - p) \quad (1)$$

where m = normalized moment (M/M_p), S_y = minor axis elastic section modulus, Z_y = minor axis plastic section modulus, c_r = residual stress ratio (σ_r/σ_y), and p = normalized axial load (P/P_y). The sign on P_y matches that of P such that p is always positive. Since this equation is based only on the accumulation of compression stresses at the end of each flange, the actual shape of the residual pattern does not affect the equation provided the maximum residual compression stress σ_r occurs at the end of the flanges. The maximum moment at which τ = 1 is maintained for major axis bending is determined in a similar manner to Eq. (1) and is found to be

$$m_1 = \frac{S_z}{Z_z}(1 - c_r - p) \quad (2)$$

where S_z = major axis elastic section modulus and Z_z = major axis plastic section modulus. Since this equation is based only on the accumulation of compression stress in the flange, the actual shape of the residual pattern does not affect Eq. (2). Two equations are needed to determine the moment and axial load conditions when τ = 0 for the minor axis bending or major axis bending conditions. For the minor axis bending condition, one equation is needed when the plastic neutral axis is inside the web thickness, and the other is needed when it is outside the web thickness.

$$\text{when } p < \frac{2\lambda_o + \lambda}{2 + \lambda}$$
$$m_0 = 1 - \frac{p^2(2 + \lambda)^2}{(2 + \lambda\lambda_o)(2 + \lambda_1)} \quad (3)$$

$$\text{when } p \geq \frac{2\lambda_o + \lambda}{2 + \lambda}$$
$$m_0 = \frac{4 - [p(2 + \lambda) - \lambda]^2}{2(2 + \lambda\lambda_o)} \quad (4)$$

where $\lambda = A_w/A_f$, $\lambda_o = t_w/b_f$ and $\lambda_1 = d_w/t_f$. For the major axis bending condition, one equation is needed when the plastic neutral axis is outside the flange thickness, and the other is needed when it is inside the flange thickness.

$$\text{when } p < \frac{\lambda}{2 + \lambda}$$
$$m_0 = 1 - \frac{p^2(2 + \lambda)^2}{4\lambda_o + \lambda(4 + \lambda)} \quad (5)$$

$$\text{when } p \geq \frac{\lambda}{2 + \lambda}$$
$$m_0 = \frac{(2 + \lambda_1)^2 - [p(2 + \lambda) - \lambda + \lambda_1]^2}{4 + \lambda_1(4 + \lambda)} \quad (6)$$

Eqs. (3)-(6) do not depend upon the shape of the residual stress pattern [7].

There is no stiffness reduction for moment and axial load conditions inside the triangular region defined by m_1. When the moment and axial load conditions are between m_1 and m_0, the stiffness reduction τ can be easily determined using Eqs. (7) and (8). Eqs. (1), (3) and (4) are used for minor axis bending, and Eqs. (2), (5) and (6) for major axis bending.

$$\text{when } p < 1 - c_r$$
$$\tau = 1 - \left(\frac{m - m_1}{m_0 - m_1}\right)^n \quad (7)$$

$$\text{when } p \geq 1 - c_r$$
$$\tau = \left(\frac{1 - p}{c_r}\right)\left(1 - \frac{m}{m_0}\right)^n \quad (8)$$

The material model allows for the independent input of the exponent n and the residual stress ratio c_r.

The residual stresses in a rotary-straightened W12 × 65 were measured by Ge and Yura [2] using the sectioning method. Based on their results, they proposed the idealized residual stress pattern given in Fig. 1. The residual compression stresses in the flanges σ_{rfc} are no longer at the ends and are significantly reduced due to the rotary-straightening process. The maximum residual tension stresses σ_{rft} are now at the flange ends and will affect the initial yield conditions under low compression load conditions. The reduced magnitude of σ_{rfc} can be easily accounted for with the appropriate value for c_r^-, but the m_1 equation now must be based on the new

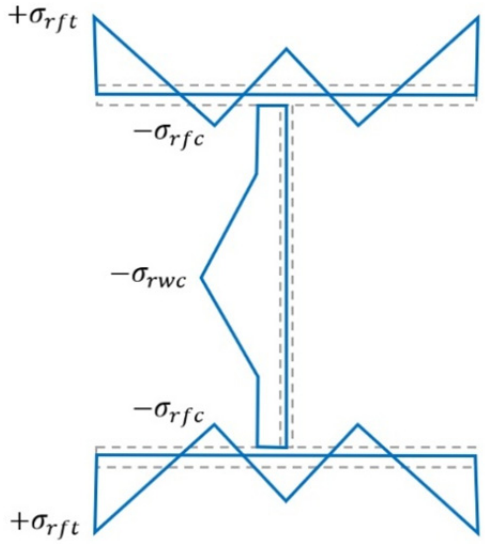

Fig. 1 Residual stress model for rotarized W-shapes.

location of σ_{rfc} at the quarter point of the flanges.

Using σ_{rfc} to calculate c_r^- in Eq. (1), the maximum moment to avoid initial compression yield with minor axis bending is given as

$$\text{when } 1 - c_r^- \geq p > 1 - 2c_r^- + c_r^+$$
$$m_1^- = \frac{2S_y}{Z_y}(1 - c_r^- - p) \tag{9}$$

Using σ_{rft} to calculate c_r^+, the maximum moment to avoid initial compression yield under moderate compression load conditions with minor axis bending is given as

$$\text{when } 1 - 2c_r^- + c_r^+ \geq p > c_r^+$$
$$m_1^{\pm} = \frac{S_y}{Z_y}(1 + c_r^+ - p) \tag{10}$$

The maximum moment to avoid initial tension yield under low compression load conditions with minor axis bending is given as

$$\text{when } c_r^+ \geq p$$
$$m_1^+ = \frac{S_y}{Z_y}(1 - c_r^+ + p) \tag{11}$$

Using σ_{rfc} to calculate c_r^- in Eq. (2), the maximum moment to avoid initial compression yield with major axis bending is given as

$$\text{when } 1 - c_r^- \geq p > \frac{c_r^+ - c_r^-}{2}$$
$$m_1^- = \frac{S_z}{Z_z}(1 - c_r^- - p) \tag{12}$$

Using σ_{rft} to calculate c_r^+, the maximum moment to avoid initial tension yield under low compression load conditions for major axis bending is given as

$$\text{when } \frac{c_r^+ - c_r^-}{2} \geq p$$
$$m_1^+ = \frac{S_z}{Z_z}(1 - c_r^+ + p) \tag{13}$$

Eqs. (1)-(8) are used for the non-rotarized material model, and Eqs. (3)-(13) are used for the rotarized material model.

3. Material Model Validation Study

The simply-supported test column conditions for the rotary-straightened W12 × 65 in Ge and Yura [2] were used to study the effectiveness of the rotarized material model. The W-shape is assumed to be fully-compact and its out-of-plane behavior fully restrained. Based on the stress magnitudes given by Ge and Yura [2] of σ_{rfc} = 5 ksi, σ_{rft} = 10 ksi and σ_y = 50 ksi, the residual stress ratios used in the study were c_r^- = 0.1 and c_r^+ = 0.2. The inelastic material model for the rotarized W12 × 65 is given in Fig. 2 for minor axis bending and in Fig. 3 for major axis bending. The effects of Eq. (9) through Eq. (13) on the yield plateau region are evident by the blue lines. Under low axial load conditions, the section yields at the flange ends under tension stress conditions (Eqs. (11) and (13)). For the minor axis bending condition, compression yield occurs at the end of the flanges with Eq. (10), and at the quarter point with Eq. (9). For major axis bending, the loss of stiffness in the web is ignored and compression yield initiates at the flange ends with Eq. (12).

Column capacity analyses were conducted in MASTAN2 [6] using a second-order inelastic analysis with constants E = 29,000 ksi, n_y = 1.2 for minor axis bending and n_z = 1.5 for major axis bending which are consistent with a previous study by Rosson [10].

The column limit load analyses for conditions of minor axis bending and major axis bending were

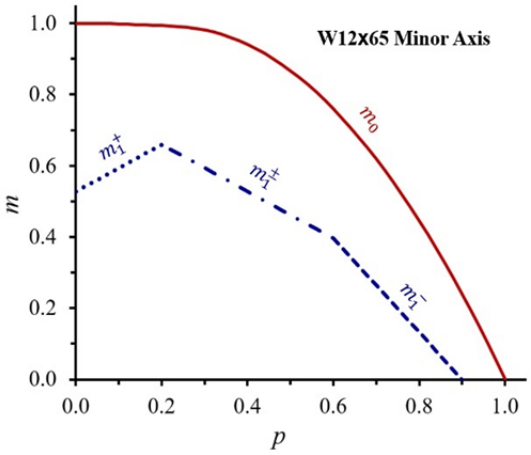

Fig. 2 m_1 and m_0 perimeter conditions for rotarized W12 × 65 material model with minor axis bending.

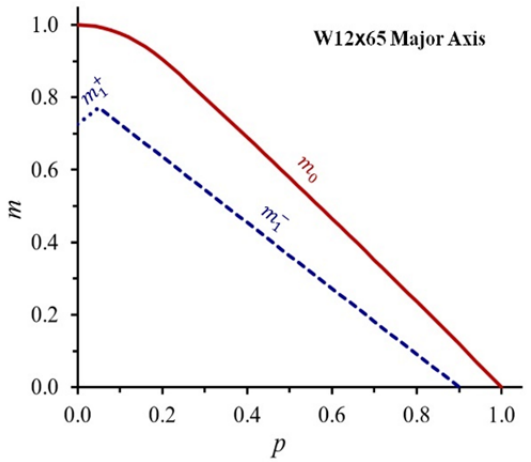

Fig. 3 m_1 and m_0 perimeter conditions for rotarized W12 × 65 material model with major axis bending.

conducted on simply-supported columns using 10 beam elements in MASTAN2 [6]. They were compared with the ABAQUS [11] column strength results by Ge and Yura [2] and the AISC (E3-2) and (E3-3) equations [12]. The results in Figs. 4 and 5 indicate very close agreement between the inelastic material models used in MASTAN2 and the more detailed ABAQUS finite element models. Due to the large $\tau = 1$ plateau regions in Figs. 2 and 3, the limit load results are considerably higher than the AISC solutions for the shorter unbraced lengths ($\lambda < 1$).

The 4-story frame depicted in Fig. 6 was modeled using MASTAN2 [6] with four beam elements per member. Second-order inelastic analyses of the frame were conducted to study the ultimate wind load conditions of the frame under increasing floor load magnitudes. To study the effects that rotary-straightened W-Shapes have on the stability of steel frames, the limit load results based on the non-rotarized material model were compared with those using the rotarized material model. The loading conditions consisted of first applying the floor loads w with a given magnitude, and then the wind loads W were applied in increments up to the ultimate value when instability occurred in the frame. The effect of the column orientation was studying by modeling all the columns with either minor axis bending or major axis bending. The initial geometric imperfection of the frame was modeled using the first eigen-mode and $L/500$ in the compounding direction.

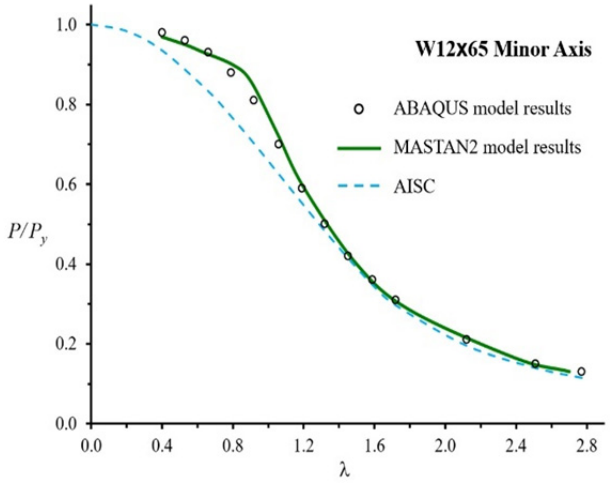

Fig. 4 Comparison of minor axis bending column results.

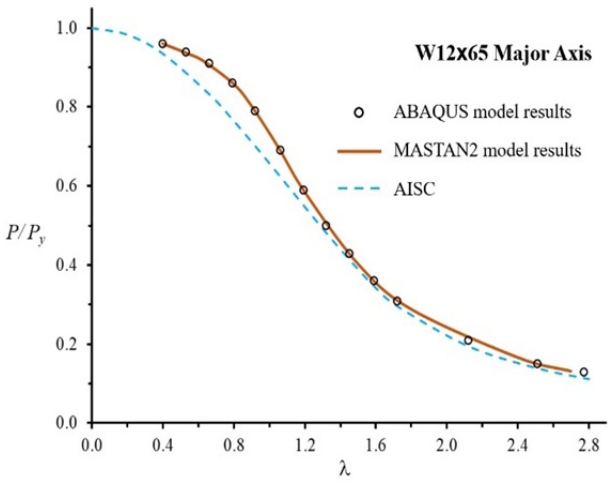

Fig. 5 Comparison of major axis bending column result.

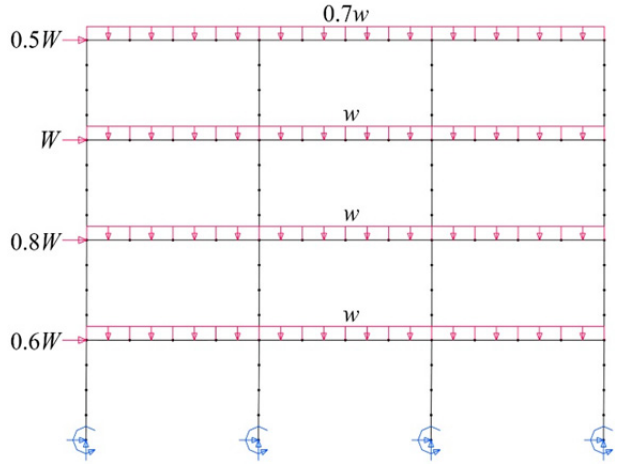

Fig. 6 MASTAN2 model of steel frame with specified wind loads and floor loads.

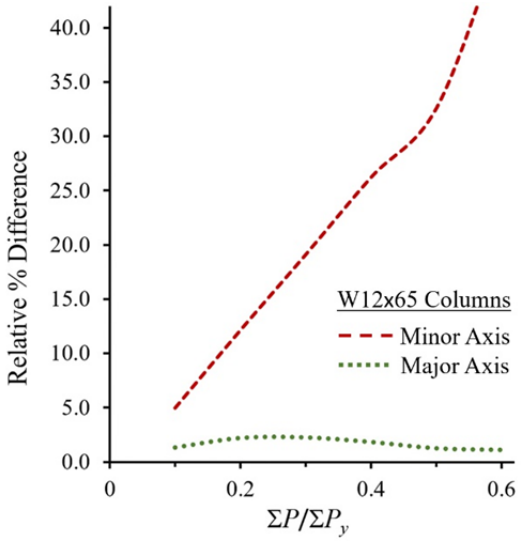

Fig. 7 Relative percent difference in maximum wind loads at different floor load magnitudes.

All the columns were modeled with the cross-section properties of a W12 × 65 with a length of 11 ft, and the beams were modeled with the properties of a W18 × 106 with a length of 20 ft. The rotarized material model used residual stress ratios of $c_r^- = 0.1$ and $c_r^+ = 0.2$, and the non-rotarized material model used a residual stress ratio of $c_r = 0.3$. All MASTAN2 analyses used E = 29,000 ksi, σ_y = 50 ksi, n_y = 1.2 for minor axis bending and n_z = 1.5 for major axis bending.

Fig. 7 illustrates the effect of rotary-straightening the W-Shapes on the ultimate wind load responses under increasing magnitude of floor loads. The x-axis is normalized by dividing the sum of the floor loads by the sum of the column yield loads ($\Sigma P/\Sigma P_y$). The y-axis is the relative percent difference in the ultimate wind load conditions for the rotarized and non-rotarized model results and is calculated as

$$Rel.\,\%\,Diff. = \frac{W_{ult}^{rot} - W_{ult}^{non}}{W_{ult}^{non}} \cdot 100\% \qquad (14)$$

where W_{ult}^{rot} = ultimate wind load condition using the rotarized material model, and W_{ult}^{non} = ultimate wind load condition using the non-rotarized material model.

For this particular frame and loading condition, the results indicate an increasingly significant difference in the modeled results as the floor loads increase when the columns are oriented with minor axis bending, but when the columns are oriented with major axis bending, there is little difference in the modeled results as the floor loads increase. Whereas Figs. 4 and 5 indicated increased capacities in the rotarized columns over the same range of λ values for both the minor axis and major axis bending conditions, the frame results in Fig. 7 indicate that the effect of rotary-straightening W-Shapes is much more significant for only the minor axis bending conditions of the columns in the steel frame.

4. Conclusions

The inelastic material model that was previously developed by the author was used to model rotary-straightened W-Shapes. Because of their unique residual stress pattern, modifications were necessary to use the existing material model. To model the rotarized W-Shapes, additional equations for the initial yield moment m_1 were required and separate c_r values were needed based on the compression residual stress σ_{rfc} and tension residual stress σ_{rft}. Validation studies compared the modeled results with those found in the literature, and it was determined that they provided similar limit load results when using the existing inelastic material models with these modifications. Rotary-straightening W-Shapes has its greatest effect on the frame capacity

when the columns are oriented with minor axis bending conditions, and this influence becomes more pronounced as the floor load magnitudes increase.

References

[1] Alpsten, G. 1972. "Residual Stresses, Yield Stress and Column Strength of Hot-Rolled and Roller-Straightened Steel Shapes." In *Proceedings of the First International Colloquium on Stability*, Paris.

[2] Ge, X., and Yura, J. A. 2019. "The Strength of Rotary-Straightened Steel Columns." In *Proceedings of the 2019 SSRC Annual Stability Conference*, St. Louis, MO.

[3] ECCS. 1984. "Ultimate Limit State Calculation of Sway Frames with Rigid Joints." *TC 8 of European Convention for Constructional Steelwork*, No. 33.

[4] Rosson, B. T. 2016. "Elasto-plastic Stress States and Reduced Flexural Stiffness of Steel Beam-Columns." In *Proceedings of the 2016 SSRC Annual Stability Conference*, Orlando, FL.

[5] Kucukler, M., Gardner, L., and Macaroni, L. 2016. "Development and Assessment of a Practical Stiffness Reduction Method for the In-Plane Design of Steel Frames." *Journal of Constructional Steel Research* 126: 187-200.

[6] Ziemian, R. D., and McGuire, W. 2020. *MASTAN2*. Version 3.5.

[7] Rosson, B. T. 2018. "Modeling the Influence of Residual Stress on the Ultimate Load Conditions of Steel Frames." In *Proceedings of the 2018 SSRC Annual Stability Conference*, Baltimore, MD.

[8] Rosson, B. T., and Ziemian, R. D. 2019. "Validation Study of a New Inelastic Material Model for Steel W-Shapes." In *Proceedings of the 2019 SSRC Annual Stability Conference*, St. Louis, MO.

[9] Rosson, B. T., and Gurneian, H. 2020. "Comparison of Inelastic Material Models Used to Determine Steel Frame Limit Load Conditions." *Journal of Civil Engineering and Architecture* 14 (2020): 61-7.

[10] Rosson, B. T., and Fadden, M. F. 2020. "Modeling the Nominal Flexural Strength of W-Shape Beams Using a New Inelastic Model." In *Proceedings of the 2020 SSRC Annual Stability Conference*, Atlanta, GA.

[11] Dassault Systèmes. Year. *ABAQUS Version 6.12-1*. Waltham, MA.

[12] ANSI/AISC 360-16. 2016. *Specification for Structural Steel Buildings*. American Institute of Steel Construction, Chicago, IL.